RSC Advances

PAPER

View Article Online
View Journal | View Issue

Cite this: *RSC Adv.*, 2022, **12**, 9044

Ni nanocatalysts supported on MIL-53(Al) for DCPD hydrogenation†

Yanan Li, Dandan Jia, Zhiping Tao* and Jie Zhao

Received 13th January 2022
Accepted 10th March 2022

DOI: 10.1039/d2ra00238h

rsc.li/rsc-advances

Metal organic frameworks (MOFs) with many unique advantages have drawn wide attention in the field of catalysis. However, the poor structural stability of MOFs limits its application. Heat treatment for MOFs can enhance its electrical conductivity and structural stability, which helps to improve the catalytic performance. Ni nanoparticles supported on MIL-53(Al) were synthesized through different heat treatment temperature. Catalysts with uniform distribution of active nickel and rich mesoporous structure were obtained by adjusting the heat treatment temperature to 500 °C. The results show this catalyst has the best hydrogenation activity and stability. Under the reaction conditions of 60 °C and 2 h, the conversion rate of DCPD is 100%, and the selectivity of *endo*-THDCPD is higher than 95%. After five cycles, the catalyst also show excellent stability and high activity, the conversion rate of DCPD is still 100%.

1. Introduction

Aerospace technology has developed rapidly since the 21st century. Therefore, increasing the speed and the range of aircraft have become problems that need to be solved urgently. The fuel system of the aircraft provides vital power for flight, it is the main factor restricting the flight of the aircraft. JP-10 (*exo*-THDCPD) is a high-density jet fuel with excellent performance. It has the advantages of large volumetric heating value, low freezing point and high density. JP-10 is widely used in cruise missiles (Tomahawk-II), supersonic aircraft, rocket propellants, *etc.*[1] Usually *exo*-THDCPD is obtained through the hydrogenation and isomerization of DCPD. Hydrogenation reaction is very important, because the incomplete hydrogenation product will cause the coking and deactivation of the catalyst during the downstream isomerization reaction, which will affect the final product.[2,3]

Currently, nickel and palladium are the commonly used active metal for DCPD hydrogenation.[4] The Pd/Al_2O_3 (ref. 5 and 6) catalyst showed high activity for DCPD hydrogenation at low temperature. Although the Pd catalyst has excellent performance in DCPD hydrogenation, the disadvantages of high price, poor toxicity resistance and easy loss, limit its large-scale application.[7] Ni catalyst is cheap and has unsatisfactory hydrogenation performance compare with Pd catalyst. The current industrialized catalyst is RANEY® Ni, which has good hydrogenation effect, but RANEY® Ni catalytic activity are unsatisfactory, prone to spontaneous combustion and difficult to recover.[8] Therefore, there is an urgent need for a catalyst with high activity and stability toward the hydrogenation of DCPD. The supported nickel catalyst has the advantages of good dispersibility and low cost. Zhang *et al.*[9] prepared $Ni/\gamma\text{-}Al_2O_3$ catalysts with nickel content of 15% and 30% and obtained the yield of *endo*-THDCPD reaching 95% and 93% when the reaction temperature is 110 °C. Sun *et al.*[10] prepared an HY molecular sieve hydrogenation catalyst loaded with nickel particles, which showed a 96% yield of *endo*-THDCPD at 170 °C. Although supported nickel-based catalysts have unique advantages, they still have the following shortcomings. One is the sintering phenomenon for the active metals due to the high heat treatment temperature. And the second is the low activity of the catalyst, which leads to high temperature of DCPD hydrogenation.[4] The high reaction temperature will cause the pyrolysis of DCPD, influence the selectivity of THDCPD.[11]

In recent years, metal organic frameworks (MOFs) have been widely used in the field of catalysis as a new type of support for various metal nanoparticles. Compared with traditional support, MOFs has the characteristics of large specific surface area, high porosity, adjustable pore size; and structural diversity.[12,13] However, due to the poor thermal stability, heat treatment for MOFs is required to improve its thermal stability. At present, MOFs has been used as precursors to synthesize carbon materials or inorganic materials with unique structures by adjusting heat treatment conditions.[14–16] The MOFs we selected here is a one-dimensional structure of MIL-53(Al), which is composed of relatively inexpensive and non-toxic aluminum as the metal cluster center and terephthalic acid as the organic ligand.[17] After heat treatment, MIL-53(Al) derivatives show excellent advancement. On the one hand, it possesses a high porosity and metal-cluster accessibility expected to favor the homogeneous dispersion of nickel species; on the other

Research Institute of Petroleum Processing, Sinopec, No. 18 Xueyuan Road, Haidian District, Beijing, China. E-mail: taozp.ripp@sinopec.com

† Electronic supplementary information (ESI) available. See DOI: 10.1039/d2ra00238h

hand, it contain organic linkers whose decomposition from heat treatment enables the formation of porosity in the catalyst.[18]

In this paper, nickel salt is loaded on MIL-53 by the impregnation method to form precursor. A series of Ni/MIL-53(Al) catalysts are prepared; by controlling the heat treatment temperature. And the hydrogenation performance of DCPD catalyzed by Ni/MIL-53(Al) has been studied. Recyclability of DCPD hydrogenation show excellent and stable performance, after cycles, the conversion rate of DCPD is 100%. The main purpose of this article is to provide some advisement for the study of a catalyst with high activity and stability.

2. Materials and methods

2.1 MIL-53(Al) preparation

All chemicals were purchased from commercial corporations and used without further treatment.

MIL-53(Al) was synthesized according to the literature.[19] 13 g of aluminum nitrate nonahydrate, 5 g of 1,4-benzenedicarboxylic acid and 50 g of deionized water were added to a 100 ml Teflon, and reacted at 220 °C for 3 days. After cooling to room temperature, the obtained white powder was then washed with deionized water and methanol, and finally dried under vacuum at 70 °C for 12 h.

2.2 Catalyst preparation

Ni/MIL-53 containing 5.0% (wt) of nickel was prepared by wetness impregnation method. $Ni(NO_3)_2 \cdot 6H_2O$ (0.1 g) solution in 4.0 ml methanol was added dropwise to the MIL-53(Al) (0.5 g) solution. The mixture was then magnetically stirred room temperature for 12 h. After rotary evaporation, the sample was dried under vacuum at 60 °C for 12 h. The catalysts were prepared by calcined in air from temperature to 300 °C, 500 °C and 700 °C for 2 h, then reduced by pure H_2 at a flow rate of 50 ml min^{-1} at the same temperature of calcination. The resulting catalysts were denoted as Ni-53-300, Ni-53-500 and Ni-53-700.

2.3 Characterization

The thermal stability of the sample was measured by the TGA/SDT-851 differential thermal analyzer of Mettler Toledo, Switzerland; the phase of the sample was measured by the 3271 X-ray fluorescence spectrometer of Kokosha Co., Ltd. of Japan; Quanta-chrome of the United States was used. The AUTOSORB-1-MP adsorption instrument is used to determine the pore structure of the sample; the JEOL JEM-2100 high-resolution transmission electron microscope is used to determine the microstructure and other information of the sample.

2.4 The hydrogenation reaction of DCPD

The hydrogenation reaction of DCPD is conducted in a stainless steel sealed autoclave with a 100 ml Teflon. Typically, 1 g DCPD was dissolved in 20 g methyl cyclohexane (solvent), and 100 mg catalyst were added to the Teflon autoclave. For remove the air in the system, H_2 was filled into the autoclave and released for three times. Then the system was charged with 3.0 MPa H_2 and heated to 60 °C under stirring and kept on reacting for 2 h. After the end of the reaction, the autoclave was cooled and pressure relief opening. The reaction liquid was analyzed by gas chromatography. The stability experimental is as follows: after one cycle of reaction, the reactant is separated from the catalyst by centrifugation, the catalyst is recovered, and then used in the next round of reaction.

3. Results and discussion

The TG curve of Ni/MIL-53(Al) is shown in Fig. 1. The TG curve of Ni/MIL-53(Al) show three stage between room temperature and 800 °C. The mass loss of step 1 before 300 °C is about 15%, which is attributed to the removal of the adsorbed solvent in the pores and the dehydration of nickel nitrate hexahydrate.[20] With the increase of temperature, the mass loss of step 2 in the temperature range of 300–420 °C is 30%, which is due to the removal of 1,4-benzenedicarboxylic acid adsorbed in the pores and the decomposition of NO^{3-} into NO_X (NO, NO_2, *etc.*)[21] When the temperature rises to 420 °C, the organic framework of MIL-53(Al) begins to collapse. There is no significant change in the curve of the temperature is 600 °C. This indicating that the organic ligands therein have been completely decomposed, this is the main loss of the MIL-53(Al), and the mass loss during step 3 is 40%.

The XRD patterns of MIL-53 (Fig. 2) match well with that reported in the literature.[22] The sharp diffraction peaks indicate that the synthesized MIL-53 has excellent crystallinity. After heat treatment, the characteristic peaks of MIL-53(Al) all changed differently and the diffraction peak of Ni (marked as "★") appeared. In Fig. 2, the peaks at 10.3°, 15.3°, and 21.4° (short dash line) are attributed to the characteristic diffraction peaks of the narrow pore framework configurations for MIL-53(Al), while the peaks at 9.0° and 12.6° (solid line) are ascribed to the characteristic diffraction peaks of the large pore framework configurations for MIL-53(Al).[23] Compared with MIL-53(Al), the XRD diffraction peaks of Ni-53-300 changes from the peaks of the narrow pore framework configurations to the peaks

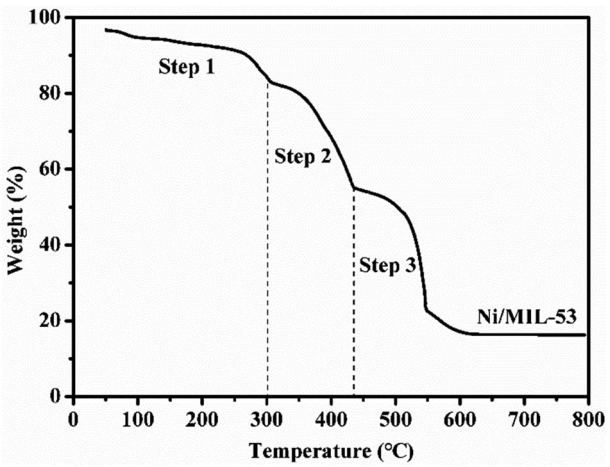

Fig. 1 TG curve of Ni/MIL-53(Al).

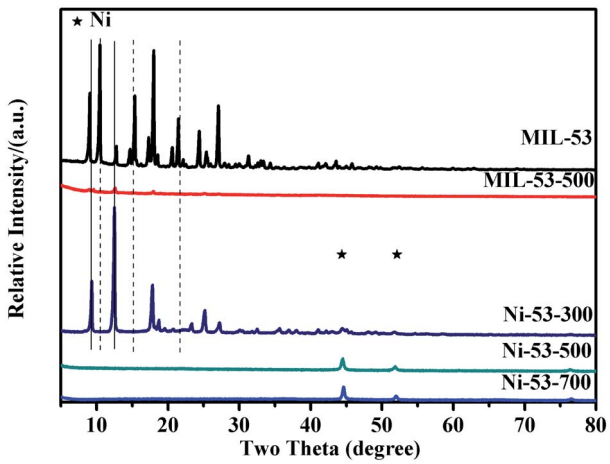

Fig. 2 X-ray diffraction patterns of MIL-53, Ni-53-300, Ni-53-500, Ni-53-700 and MIL-53-500.

of the large pore framework configurations. Because MIL-53(Al) has a flexible structure, that is, the size of the pores will change with the "breathing behavior", and the corresponding XRD patterns will also change accordingly.[24] The two kinds of pore structures for MIL-53(Al) have the same chemical composition and topological structure, but the size of the pores has changed to a certain extent.[25] This is also the special structural feature of MIL-53(Al) with a flexible framework. When the heat treatment temperature is 300 °C, the molecules in the pores are removed, so that the narrow pore structure of MIL-53(Al) is converted into the large pore structure of MIL-53(Al), and this will also be explained in the BET characterization. There is no diffraction peaks at 0–30° in Fig. 2 The high heat treatment temperature of Ni-53-500 and Ni-53-700 may cause the structure of MIL-53(Al) transform into an amorphous form of Al_2O_3.[26] However, Fig. 2 shows the XRD spectra of MIL-53(Al) before and after calcination at 500 °C. It can be seen that MIL-53-500 still retains the characteristic structure of MIL-53(Al) which may be extremely weak.

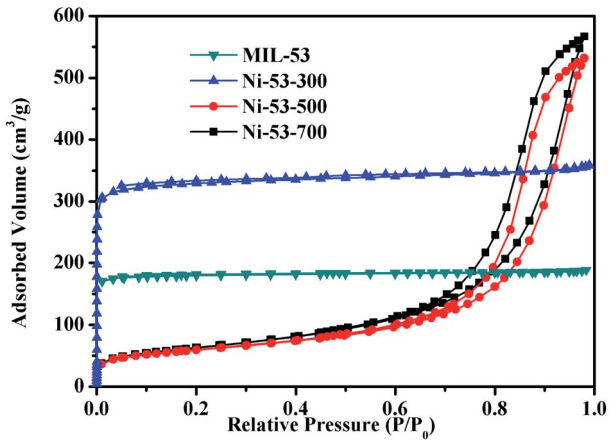

Fig. 3 N_2 adsorption–desorption isotherms of MIL-53, Ni-53-300, Ni-53-500 and Ni-53-700.

Table 1 Textural properties of the samples

Sample	S_{BET} ($m^2\ g^{-1}$)	$S_{External}$ ($m^2\ g^{-1}$)	Pore volume ($cm^3\ g^{-1}$)	Pore size (nm)
MIL-53	602	12	0.29	1.9
Ni-53-300	1260	50	0.54	2.7
Ni-53-500	211	206	0.82	15.5
Ni-53-700	224	220	0.78	14.6

The N_2 adsorption–desorption isotherms of the MIL-53(Al) and catalysts are displayed in Fig. 3. The isotherms of MIL-53(Al) and Ni-53-300 show the type I curves, indicating that they are a typical microporous material. Due to the above-mentioned "breathing behavior", the pore size of Ni-53-300 will be slightly larger than the natural state of MIL-53(Al). With the heat treatment temperature is 300 °C, the molecules adsorbed in the pores due to the "breathing behavior" are removed, so the adsorption capacity of Ni-53-300 will be larger than that of MIL-53(Al). All of the above indicate that the special structure of the MIL-53(Al) was not decomposed when calcined at 300 °C, which can also be explained by XRD (Fig. 2). The isotherms of Ni-53-500 and Ni-53-700 all show the type IV curves, with an apparent hysteresis loop of H1 in the relative pressure (P/P_0) range of 0.5–1.0.[27] This result indicates that the microporous structure of MIL-53(Al) is destroyed due to the pyrolysis of the organic ligands under the high heat treatment temperature, resulting in a new mesoporous structure. It is worth noting that the H1 hysteresis loop of Ni-53-500 is slightly narrower than Ni-53-700 and shifted to the higher pressure area, the data in Table 1 also indicates that the pore size 15.5 nm of Ni-53-500 will be slightly larger than that 14.6 nm of Ni-53-700. After all, catalysts with different types of pores were obtained through heat treatment at different temperatures. The pore size of Ni-53-500 is the largest of the kinds of catalysts. The large pore can also promote the catalytic reaction and the facilitate diffusion of reactant molecules, this may decline the DCPD hydrogenation reaction temperature.

Fig. 4 shows the morphologies of Ni-53-300, Ni-53-500 and Ni-53-700. And corresponding Ni particle size distribution can be seen in the Fig. S1.† It can be seen in Fig. 4(a) that the Ni particles of Ni-53-300 are highly dispersed, and the average size of the particles is 4–6 nm. In Fig. 4(b), due to the increase of the heat treatment temperature, the Ni particles of Ni-53-500 have slightly aggregated, and the average size of the particles is 15–25 nm. Continue to increase the heat treatment temperature,

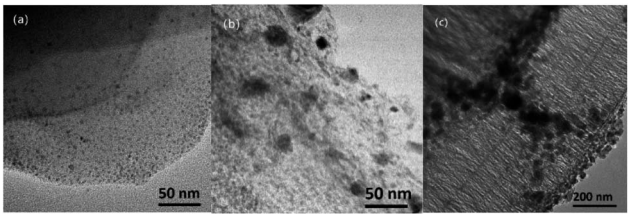

Fig. 4 TEM images of (a) Ni-53-300, (b) Ni-53-500 and (c) Ni-53-700.

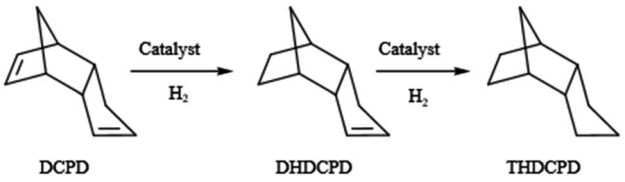

Fig. 5 Schematic representation for hydrogenation of dicyclopentadiene.

resulting in a serious aggregation of Ni-53-700 Ni particles, the average size of the nickel particles is 30–40 nm with poor dispersion. These can also be proved by Sherrer equation of XRD patterns in Fig. S3.† These indicate the nickel particles size become larger with the increase heat treatment temperature.

4. Catalytic performance

The reaction consists of typical consecutive steps: (1) DCPD hydrogenation into DHDCPD (2) THDCPD is obtained by further hydrogenation of DHDCPD (Fig. 5). DCPD chemical structure have two unsaturated double bonds. One double bond is the in cyclopentene ring (CP-bond) and the other is the double bond in norbornene ring (NB-bond). The NB-bond is thermodynamically less stable due to greater strain and is likely to be more easily hydrogenated. NB-bond is more easily saturated than CP-bond in the hydrogenation process. As a result, the majority of the hydrogenation intermediate is DHDCPD.[28]

The hydrogenation performance of different catalyst is evaluated and shown in Fig. 6. All catalysts show excellent performance of catalytic DCPD hydrogenation. The DCPD conversion and THDCPD selectivity are above 98% catalyzed by Ni-53-500 and Ni-53-700. The DCPD conversion is above 99% and THDCPD selectivity is 92% catalyzed by Ni-53-300. However, the recyclability is a very important character for practical application. The poorly stable catalyst has a short service life, which seriously affects its application in industrial production. Therefore, it is more important to investigate the stability of the catalyst.

It can be seen from Fig. 7(a and b) that under the first cycle, the conversion of DCPD is above 98% and the selectivity of THDCPD is 92% for the Ni-53-300 catalyst. But after the second cycle, the conversion of DCPD catalyzed by Ni-53-300 is only 5.9%, and the product is almost DHDCPD. After the third cycle, conversion of DCPD and selectivity of THDCPD almost to zero. The poor catalytic stability of Ni-53-300 may be attributed to the following points: due to the low heat treatment temperature, it can be found in the Fig. 4(a) that the Ni particles are well dispersed, the original special pore structure of the MIL-53(Al) can also be retained (XRD in Fig. 2 and the BET in Fig. 3). However, the special pore structure with the "breathing behavior" of MIL-53(Al) can cause some molecules to accumulate in the pores after the reaction, making it difficult for the reactants to diffusion in the pores. The catalyst after the reaction, characteristic diffraction peaks with the same small framework properties as MIL-53(Al) appeared at 10.3°, 15.3°,

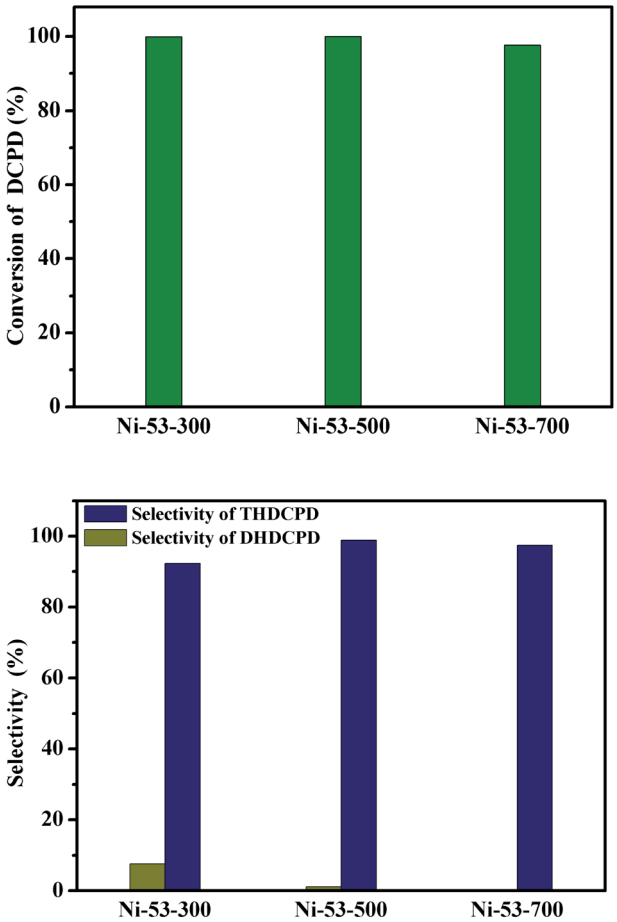

Fig. 6 DCPD hydrogenation catalyzed by different catalysts: Ni-53-300; Ni-53-500; Ni-53-700.

and 21.4° in Fig. 8(d). And the BET of Ni-53-300 after reaction decreased seriously (Fig. 7(c)). All this evidence indicates that the pores may be blocked due to the "breathing behavior" of MIL-53(Al), which reduces the hydrogenation activity of DCPD. So, the recyclability of DCPD hydrogenation catalyzed by Ni-53-300 is less than satisfactory.

H_2-TPR experiments are carried out to investigate metal–support interaction and the reduction characteristics of the catalysts. H_2-TPR curves of all the catalysts have been shown in Fig. S2.† The H_2-TPR test of Ni-53-300 was repeated several times. During the heating process of Ni-53-300 at 400 °C in the H_2-TPR test, volatile substances were generated due to the decomposition of MIL-53, which blocked the test instrument and caused the curve to be interrupted, as shown in Fig. S2a.† For Ni-53-300, the main peak is at about 350 °C, and a shoulder peak is at about 280 °C. Ni-53-500 has a peak at 280 °C. Ni-53-700 has a peak at about 350 °C. This all indicate the two different interactions between nickel oxide particles and the support.[29]

The conversion of DCPD and the selectivity of THDCPD are all 100% for the Ni-53-500 and Ni-53-700 catalysts under the first cycle. After the second cycle, the conversion of DCPD

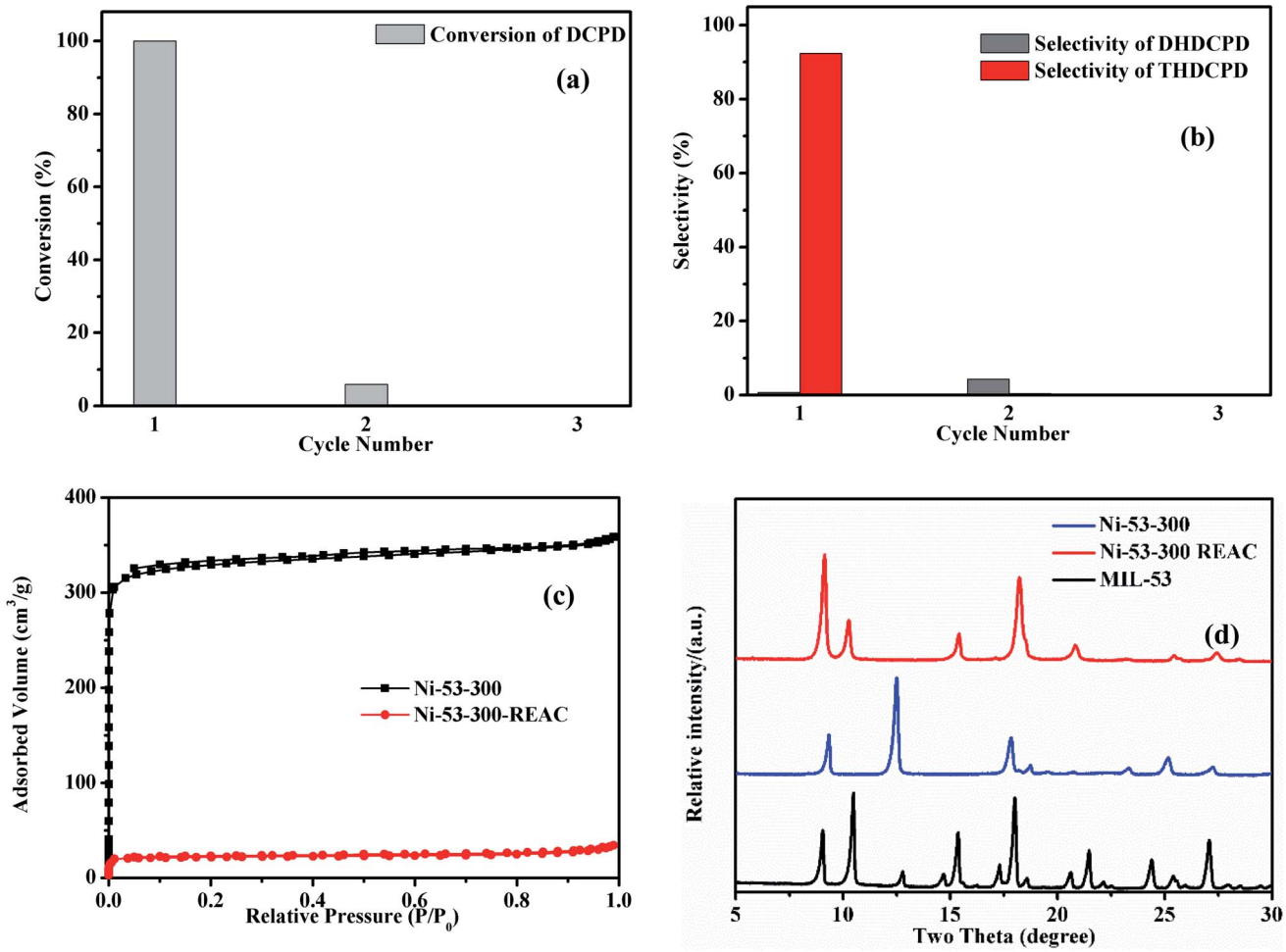

Fig. 7 (a and b) Recyclability of DCPD hydrogenation catalyzed by Ni-53-300 (c) N_2 physisorption isotherms of Ni-53-300 before and after reaction (d) X-ray diffraction patterns of MIL-53(Al) and Ni-53-300 before and after reaction.

catalyzed by Ni-53-500 and Ni-53-700 are both above 98%, but the selectivity of THDCPD of catalyzed by Ni-53-700 is higher than Ni-53-500. After the third cycle, the conversion of DCPD catalyzed by Ni-53-500 is 100% and the selectivity of THDCPD is 60.8%. The conversion of DCPD catalyzed by Ni-53-700 is also 100% and the selectivity of THDCPD is 18.7%. And selectivity of THDCPD catalyzed by Ni-53-500 is higher than that of Ni-53-700, which is much lower than the second cycle. After the fourth and fifth cycles, the conversion of DCPD catalyzed by Ni-53-500 is still 100%, but the selectivity of THDCPD is reduced to 38.1%. However, the conversion of DCPD catalyzed by Ni-53-700 decreased to 70.7%, and selectivity of THDCPD also decline seriously, became 1.7%. The difference in catalytic performance of the catalysts may be attributed to the following points. Generally, the pore size and active particle distribution all have a great influence on the catalytic effect. The active metal distribution of Ni-53-300 catalyst is better than Ni-53-500 and Ni-53-700 catalyst. But under the heat treatment temperature of 500 °C and 700 °C, Ni-53-500 and Ni-53-700 catalyst produced mesoporous pores, which play an important role in the diffusion of the reaction. Ni-53-500 and Ni-53-700 have better catalytic DCPD hydrogenation effects than Ni-53-300. From the TG curve in Fig. 1, it can be seen that the framework of the MIL-53(Al) collapse when heat treatment temperature is 440 °C. The BET in Fig. 3 shows that Ni-53-500 and Ni-53-700 have become mesoporous material, which make the reactant and product molecules freely diffusion. The XRD of Ni-53-500 in Fig. 2 show that the structure of Ni-53-500 may be amorphous Al_2O_3. Therefore, Ni-53-500 have a part of MIL-53(Al) structure in TG curve of Fig. 1. It can be seen in the TEM of Fig. 4 that the Ni particles of Ni-53-500 is 15–25 nm, Ni-53-700 is about 30–40 nm. So, Ni-53-700 nickel particles has a serious aggregation compared with Ni-53-500.

Therefore, under the same cycle conditions, Ni-53-500 has the best effect in catalyzing DCPD to THDCPD, followed by Ni-53-700, and Ni-53-300 is the worst. Although Ni particles of Ni-53-300 are highly dispersed, the special framework of catalyst cause some molecules to accumulate in the pores. Ni-53-500 and Ni-53-700 have mesoporous pores, this can make molecules freely diffusion and contact with active metal. All results indicate that the pore structure of the catalyst make the most important impact on DCPD hydrogenation.

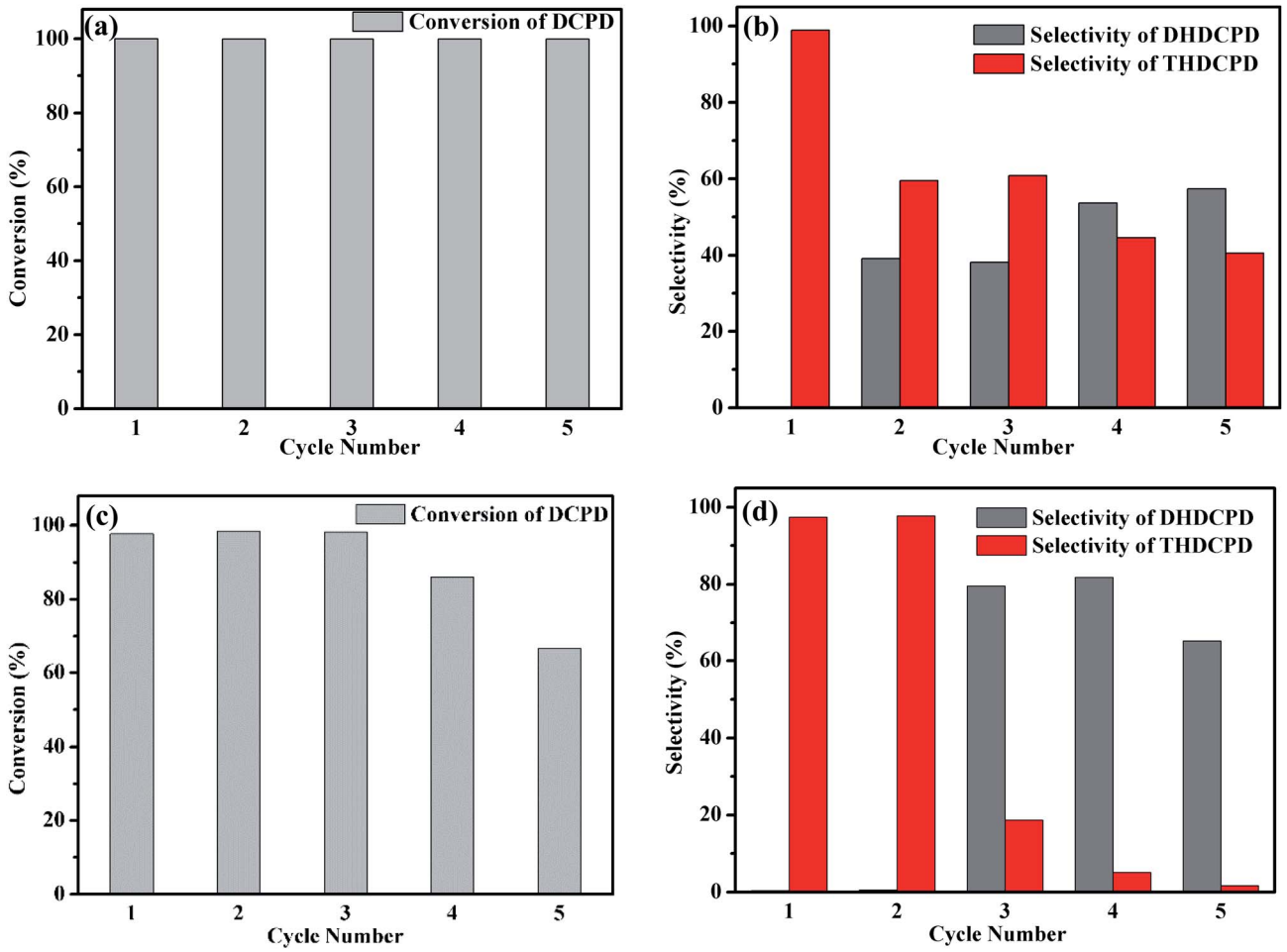

Fig. 8 Recyclability of DCPD hydrogenation catalyzed by different catalysts: (a and b) Ni-53-500; (c and d) Ni-53-700.

5. Conclusions

In summary, we prepared a series of highly active catalysts using Ni/MIL-53 as a precursor *via* controlled heat treatment temperature. The heat treatment temperature have a great influence on catalyst structure and nickel particles dispersion. It is demonstrated that all catalysts exhibited high activity in the hydrogenation of DCPD. Ni-53-500 catalyst presents the excellent performance and outstanding recyclability in the hydrogenation of DCPD to THDCPD, which can be attributed to the high Ni distribution and large pore size. This work highlights the influence of the heat treatment on Ni/MOF catalysts. It might bring new opportunities in the researches of DCPD hydrogenation. We believe that this approach can be further extended to various types of MOFs consisting of other metals and will be expanded to other related fields.

Conflicts of interest

There are no conflicts to declare.

Acknowledgements

We thank the support of National Key R&D Program of China (2021YFB3500700) for financial support.

Notes and references

1 E. Xiu-tian-feng, X. Zhi, Y. Zhang, C. Li, J.-J. Zou, X. Zhang and L. Wang, *Chem. Eng. Sci.*, 2015, **129**, 9–13.
2 P. Tamizhdurai, A. Ramesh, P. S. Krishnan, V. Mangesh, S. Umasankar, S. Narayanan, C. Ragupathi and K. Shanthi, *Microporous Mesoporous Mater.*, 2019, **290**, 109678.
3 Y. Wang, G. Luo, X. Xu and J. Xia, *Catal. Commun.*, 2014, **53**, 15–20.
4 Z. Fang, D. Shi, N. Lin, A. Li, Q. Wu, Q. Wang, Y. Zhao, C. Feng, Q. Jiao and H. Li, *Appl. Catal., A*, 2019, **574**, 60–70.
5 G. Liu, Z. Mi, L. Wang, X. Zhang and S. Zhang, *Ind. Eng. Chem. Res.*, 2006, **45**, 8807–8814.
6 G. Liu, X. Zhang, L. Wang, S. Zhang and Z. Mi, *Chem. Eng. Sci.*, 2008, **63**, 4991–5002.

7 N. Sadokhina, G. Smedler, U. Nylén, M. Olofsson and L. Olsson, *Appl. Catal., B*, 2018, **236**, 384–395.
8 W. C. Cheng, L. J. Czarnecki and C. J. Pereira, *Ind. Eng. Chem. Res.*, 1989, **28**, 1764–1767.
9 Z. Yu, X. Bing, X. Jie and L. Yongxin, *Spec. Petrochem.*, 2011, **28**, 21–24.
10 S. Congming and L. Gang, *Acta Pet. Sin., Pet. Process. Sect.*, 2012, **28**, 296.
11 Y. Pan, H. Zhang, C. Zhang, H. Wang, K. Jing, L. Wang, X. Zhang and G. Liu, *Energy Fuels*, 2020, **34**, 1627–1638.
12 G. Férey, *Chem. Soc. Rev.*, 2008, **37**, 191–214.
13 M. Eddaoudi, D. B. Moler, H. Li, B. Chen, T. M. Reineke, M. O'keeffe and O. M. Yaghi, *Acc. Chem. Res.*, 2001, **34**, 319–330.
14 D. Yuan, J. Chen, S. Tan, N. Xia and Y. Liu, *Electrochem. Commun.*, 2009, **11**, 1191–1194.
15 X. Yan, N. Lu, B. Fan, J. Bao, D. Pan, M. Wang and R. Li, *CrystEngComm*, 2015, **17**, 6426–6433.
16 Y. Lü, W. Zhan, Y. He, Y. Wang, X. Kong, Q. Kuang, Z. Xie and L. Zheng, *ACS Appl. Mater. Interfaces*, 2014, **6**, 4186–4195.
17 V. Finsy, L. Ma, L. Alaerts, D. De Vos, G. Baron and J. Denayer, *Microporous Mesoporous Mater.*, 2009, **120**, 221–227.
18 Z. Li, Y. n. Wu, J. Li, Y. Zhang, X. Zou and F. Li, *Chem.–Eur. J.*, 2015, **21**, 6913–6920.
19 L. Hamon, C. Serre, T. Devic, T. Loiseau, F. Millange, G. r. Férey and G. D. Weireld, *J. Am. Chem. Soc.*, 2009, **131**, 8775–8777.
20 L. Brewer and P. R. Wengert, *Metall. Trans.*, 1973, **4**, 83–104.
21 S. Yuvaraj, L. Fan-Yuan, C. Tsong-Huei and Y. Chuin-Tih, *J. Phys. Chem. B*, 2003, **107**, 1044–1047.
22 T. Loiseau, C. Serre, C. Huguenard, G. Fink, F. Taulelle, M. Henry, T. Bataille and G. Férey, *Chem.–Eur. J.*, 2004, **10**, 1373–1382.
23 T. Rodenas, M. Van Dalen, E. García-Pérez, P. Serra-Crespo, B. Zornoza, F. Kapteijn and J. Gascon, *Adv. Funct. Mater.*, 2014, **24**, 249–256.
24 T. K. Trung, P. Trens, N. Tanchoux, S. Bourrelly, P. L. Llewellyn, S. Loera-Serna, C. Serre, T. Loiseau, F. Fajula and G. Férey, *J. Am. Chem. Soc.*, 2008, **130**, 16926–16932.
25 N. Ramsahye, G. Maurin, S. Bourrelly, P. Llewellyn, T. Loiseau and G. Ferey, *Phys. Chem. Chem. Phys.*, 2007, **9**, 1059–1063.
26 S. Shi, S. Qian, X. Hou, J. Mu, J. He and X. Chou, *Adv. Condens. Matter Phys.*, 2018, **2018**, 1–10.
27 J. Meija, T. B. Coplen, M. Berglund, W. A. Brand, P. De Bièvre, M. Gröning, N. E. Holden, J. Irrgeher, R. D. Loss and T. Walczyk, *Pure Appl. Chem.*, 2016, **88**, 293–306.
28 J.-J. Zou, X. Zhang, J. Kong and L. Wang, *Fuel*, 2008, **87**, 3655–3659.
29 Y. Chen and J. Chen, *Appl. Surf. Sci.*, 2016, **387**, 16–27.